PAPER

A composite hydrogel-3D printed thermoplast osteochondral anchor as example for a zonal approach to cartilage repair: *in vivo* performance in a long-term equine model

Biofabrication

PAPER

A composite hydrogel-3D printed thermoplast osteochondral anchor as example for a zonal approach to cartilage repair: *in vivo* performance in a long-term equine model

I A D Mancini[1,2,6], S Schmidt[3], H Brommer[1], B Pouran[4], S Schäfer[5], J Tessmar[5], A Mensinga[4], M H P van Rijen[4], J Groll[5], T Blunk[3], R Levato[4], J Malda[1,2,4] and P R van Weeren[1,2,6]

[1] Department of Clinical Sciences, Faculty of Veterinary Medicine, Utrecht University, Yalelaan 112, 3584CM, Utrecht, The Netherlands
[2] Regenerative Medicine Utrecht, Utrecht University, Utrecht, The Netherlands
[3] Department of Trauma, Hand, Plastic and Reconstructive Surgery, University of Würzburg, Würzburg, Germany
[4] Department of Orthopedics, University Medical Center Utrecht, Utrecht University, Utrecht, The Netherlands
[5] Department of Functional Materials in Medicine and Dentistry and Bavarian Polymer Institute, University of Würzburg, Würzburg, Germany
[6] Author to whom any correspondence should be addressed.

E-mail: mancini.vet@gmail.com **and** r.vanweeren@uu.nl

Keywords: zonal composite scaffolds, osteochondral repair, equine animal model, articular cartilage progenitor cells, bone and cartilage tissue engineering

Supplementary material for this article is available online

RECEIVED
13 July 2019

REVISED
14 April 2020

ACCEPTED FOR PUBLICATION
20 May 2020

PUBLISHED
29 June 2020

Abstract

Recent research has been focusing on the generation of living personalized osteochondral constructs for joint repair. Native articular cartilage has a zonal structure, which is not reflected in current constructs and which may be a cause of the frequent failure of these repair attempts. Therefore, we investigated the performance of a composite implant that further reflects the zonal distribution of cellular component both *in vitro* and *in vivo* in a long-term equine model. Constructs constituted of a 3D-printed poly(ε-caprolactone) (PCL) bone anchor from which reinforcing fibers protruded into the chondral part of the construct over which two layers of a thiol-ene cross-linkable hyaluronic acid/poly(glycidol) hybrid hydrogel (HA-SH/P(AGE-co-G)) were fabricated. The top layer contained Articular Cartilage Progenitor Cells (ACPCs) derived from the superficial layer of native cartilage tissue, the bottom layer contained mesenchymal stromal cells (MSCs). The chondral part of control constructs were homogeneously filled with MSCs. After six months *in vivo,* microtomography revealed significant bone growth into the anchor. Histologically, there was only limited production of cartilage-like tissue (despite persistency of hydrogel) both in zonal and non-zonal constructs. There were no differences in histological scoring; however, the repair tissue was significantly stiffer in defects repaired with zonal constructs. The sub-optimal quality of the repair tissue may be related to several factors, including early loss of implanted cells, or inappropriate degradation rate of the hydrogel. Nonetheless, this approach may be promising and research into further tailoring of biomaterials and of construct characteristics seems warranted.

1. Introduction

Osteochondral lesions, i.e. those involving both the articular cartilage and subchondral bone, may lead to tissue degeneration that can progress into osteoarthritis (OA) [1]. In clinics, a commonly applied strategy for (osteo)chondral repair relies on the recruitment of native repair cells through microfracture [2]. More sophisticated techniques include different forms of mosaicplasty [3] and implantation of osteochondral allografts [4]. Clinical trials have also used various commercially available scaffolds [5, 6], with or without cells.

However, these strategies are often associated with significant limitations, like donor site morbidity and high costs [7] and all result in insufficient functional repair [8].

The failure to achieve successful chondral repair may be due to the avascular nature of articular cartilage [9]. Recent research has focused on the generation of living personalized prostheses for joint repair through biofabrication techniques [10, 11], however, the resulting repair tissue still lacks the hierarchical collagen structure typical of healthy native articular cartilage [12]. This results in formation of repair tissue that is biomechanically inferior, contributing to failure of function in the long-term [13]. Restoration of the bone part in osteochondral repair is less challenging, because of the innate repair response of bone [14], which is a well vascularized tissue. This discrepancy in intrinsic healing capacities between bone and cartilage makes the production of constructs for osteochondral defect repair a complex task, as it requires a highly specialized multiphasic scaffold to mimic the functional characteristics of the native osteochondral unit [15].

Tissue engineering techniques have the potential, through the use of multiple materials and cell types, to further approximate the zonal architecture of the native tissue [16, 17]. To achieve this, appropriate choices need to be made with respect to both the biomaterials and the cells that are used. Hydrogels are considered promising biomaterials for cartilage repair because of their intrinsic hydrated nature. Also, they can be functionalized by incorporation of chemical cues, providing them a high degree of versatility for biofabrication applications, including replication of spatially organized constructs [11, 18]. However, a definite drawback is that their stiffness is very limited, making them unsuitable to recreate the mechanical characteristics of the native tissue on their own [14]. A key challenge for successful regeneration is the choice of the biomaterials used to build a bio-inspired multiphasic zonally-organized construct [19]. In such constructs, hydrogels based on synthetic polymers, such as polyglycidols-based (PG) polymers [20] combined with a thiol-functionalized hyaluronic acid (HA-SH) [21], may offer the possibility to provide a cell-friendly environment while still permitting control of the chemical and physical properties [22].

To increase chances of success, it is also possible to improve the biomechanical performance of hydrogels by combining biomaterials with fiber reinforcements, although fiber thickness and deposition patterns have different effects on biomechanics [23], hence this principle was also adapted for this study. The combination of biomaterials and fiber reinforcement however, may be insufficient, as the regeneration is also driven by cells [24], partially through their interaction upon implantation with the host environment [25]. There is, however, still debate on which cell type may give optimal results for regenerative purposes [22, 26].

To assess if the appropriate choices have been made, a pre-requisite for eventual clinical application is the long-term evaluation in a reliable large animal model [27]. The equine model has often been described as a suitable option for this purpose, as the equine stifle has characteristics that resemble those of the human knee, and an equally, possibly more challenging mechanical environment [27, 28].

Chondrocytes have been used with some success in the equine model [29, 30], as have bone-marrow derived stem cells (MSCs), which, however, showed limited improvement in repair compared to control treatments in the long-term [31], and are known to exhibit a hypertrophic phenotype under chondrogenic induction [32]. A relatively unexplored cell population identified in the superficial layer of cartilage, known as Articular Cartilage Progenitor Cells (ACPCs) [33], may be more suitable than MSCs [34]. These cells show multipotent capacity for differentiation, as do MSCs, and *in vitro*, they synthesize collagen type II and aggrecan, but no collagen type X, marker of hypertrophic chondrocytes [35]. These cells also lack RUNX2, a master transcription factor for osteogenic differentiation observed during endochondral ossification [36]. Additionally, ACPCs harvested from the equine articular cartilage have been thoroughly characterised. In particular, gene expression analysis showed positivity of ACPCs for CD73, CD90, and CD105, negativity for hematopoietic marker CD34 and leukocyte marker CD45. ACPCs were also shown to be positive for CD29, CD44, CD49, CD106 and CD166 [24].

Furthermore, when embedded in a gelatin-based hydrogel, ACPCs were found to express PRG4, a gene that encodes production of lubricin in the superficial layer of cartilage [37], indicating that these cells represent a promising cell source for cartilage repair, and may instruct repair cells to develop a superficial zone phenotype [38], making them great candidates for attempting to recapitulate the zonal features of native cartilage. The principle of differences in spatial distribution to enhance chondral formation has been previously investigated with different cell sources such as chondrocytes [39], MSCs and ACPCs [24]. In the study by Levato *et al* in particular, the *in vitro* combination of the two latter cell types appeared the most promising [24].

Therefore, here we investigate the performance of a multi-composite implant for the repair of osteochondral defects, focusing on the possible effect of a zonal distribution of the cellular component. A composite construct with zonal cell distribution was developed utilizing MSCs and ACPCs. The basic construct consisted of a thiol-ene cross-linkable hyaluronic acid/poly(glycidol) hybrid hydrogel (HA-SH/P(AGE-co-G)) [21] and a 3D-printed poly(ε-caprolactone) (PCL) osteochondral anchor previously tested for fixation [40] in the equine model. We evaluate the impact of a zonal

configuration against a non-zonal configuration *in vitro* and *in vivo* in a long-term equine model for cartilage repair, as well as the long-term effects of the anchoring scaffold for bone repair.

2. Materials and methods

2.1. Isolation and culture of cells

2.1.1. Cell expansion for in vitro experiments

Equine MSCs and ACPCs were isolated as described by Levato *et al* from two different donors (one for cell type) [24]. These cells were used for three independent experiments, in which they were cultured up to passage 4 in expansion medium. For MSCs this was DMEM high glucose 4.5 g l^{-1} (Sigma-Aldrich, St. Louis, MO, USA), supplemented with 10% FCS (Thermo Fisher, Waltham, USA), 1 ng ml^{-1} bFGF (Recombinant Human FGF-basic/145aa, BioLegend, London, UK) and 1% P/S (100 U ml^{-1} penicillin, 0.1 mg ml^{-1} streptomycin, Thermo Fisher, Waltham, USA). For ACPCs: DMEM high glucose 4.5 g l^{-1}, supplemented with 10% FCS, 1% MEM NEAA (Thermo Fisher, Waltham, USA), 0.2 mM L-ascorbic acid 2-phosphate (Sigma-Aldrich, St. Louis, MO, USA), 5 ng ml^{-1} bFGF and 1% P/S.

2.1.2. Cell encapsulation in HA-SH/P(AGE-co-G) hydrogels for in vitro experiments

For hydrogel preparation, HA-SH (5 wt%), P(AGE-co-/G) (5 wt%), and the photoinitiator I2959 (0.05 wt%, BASF, Ludwigshafen, Germany) were dissolved in PBS (Thermo Fisher, Waltham, USA) [21]. The pH of the slightly acidic solution was neutralized using 5 M NaOH (Sigma-Aldrich, St. Louis, MO, USA). Subsequently, MSCs or ACPCs at passage 4 were suspended in the precursor solution (20×10^6 cells ml^{-1}), and the cell suspension was cast in cylindrical silicone molds with a diameter of 6 mm. Constructs containing either MSCs or ACPCs alone had a volume of 55 μl and were crosslinked via UV irradiation at 365 nm for 10 min. For zonal constructs, 35 μl MSC suspension was first irradiated for 5 min; then, 20 μl ACPC suspension was pipetted on top and irradiated again for 5 min to complete crosslinking. Pure hydrogel constructs (without PCL) were used for *in vitro* experiments. Constructs were cultured for 28 d in chondrogenic differentiation medium (DMEM high glucose, supplemented with 1% v/v ITS + premix (Corning, NY, USA), 0.2 mM L-ascorbic acid-2-phosphate, 100 nM dexamethasone (Sigma-Aldrich, St. Louis, MO, USA), 10 ng ml^{-1} TGF-β1 (BioLegend, London, UK), 1% P/S). Per construct, 1 ml medium was used and refreshed every 2–3 d. For *in vitro* evaluation, three independent experiments were conducted. For each experiment, the number of samples per group was (n) equals 3.

2.2. Generation of constructs for in vivo study

2.2.1. Osteochondral constructs

2.2.1.1. Osteochondral anchor.

Osteochondral anchors were fabricated as previously described in Mancini *et al* [40]. Briefly, a screw-based extruder on a 3DDiscovery printer (regenHU SA, Switzerland) was used to 3D print GMP-grade PCL (Purasorb® PC 12, Corbion, The Netherlands). The osteochondral plug was designed using BioCAD software (regenHU SA) as a cylinder with 6 mm diameter, featuring a square-grid scaffold structure with six zones with different porosities. The design was replicated with decreasing porosity to mimic transition from trabecular to subchondral bone, resulting in a virtually closed interface between the chondral and osteal compartments, and a chondral fiber reinforcement to enhance fixation of biomaterials and increase biomechanical resistance [40]. The scaffold also allowed for press-fit fixation of the implant.

2.2.1.2. Cell encapsulation in HA-SH/P(AGE-co-G) hydrogels.

Cell encapsulation was, in principle, executed as described above, using cells from the same donors (section 2.1). The HA-SH/P(AGE-co-G) hydrogel/cell mixture was cast in a layer-wise fashion on top of the 3D-printed PCL osteochondral scaffold. Zonal architecture was determined by subsequent casting of two hydrogel layers with different cell types, while non-zonal constructs were constituted of a single layer of hydrogel laden with a single cell-type. Specifically, for the chondral portion of the constructs a single layer was cast with 55 μl of hydrogel mixed with equine MSCs (20×10^6 cells ml^{-1} of hydrogel) for the non-zonal constructs. For the zonal constructs, two hydrogel layers seeded with equine MSCs (35 μl, 20×10^6 cells ml^{-1} of hydrogel) and with chondroprogenitor cells (20 μl, 20×10^6 cells ml^{-1} of hydrogel) were consecutively cast on the osteochondral anchor (figure 1). Constructs were stored in differentiation medium (see paragraph 2.1.2) overnight and soaked with DMEM high glucose with no additions before implantation.

2.3. Evaluation of chondrogenesis *in vitro*

2.3.1. Biochemical analysis

After 28 d, constructs (n = 3) were harvested and DNA, GAG and hydroxyproline content was measured [41]. Briefly, a TissueLyser (Quiagen, Hilden, Germany) was used to homogenize samples at 25 Hz for 5 min and afterwards samples were digested in a papain solution (3 U ml^{-1}) for 16 h at 60 °C. DNA content was measured fluorometrically using Hoechst 33 258 DNA intercalating dye (Ex: 360 nm, Em: 460 nm), with salmon testes DNA as a standard [42]. GAG content was determined by DMMB assay at 525 nm, using bovine chondroitin sulfate as a standard [43]. The amount of hydroxyproline was

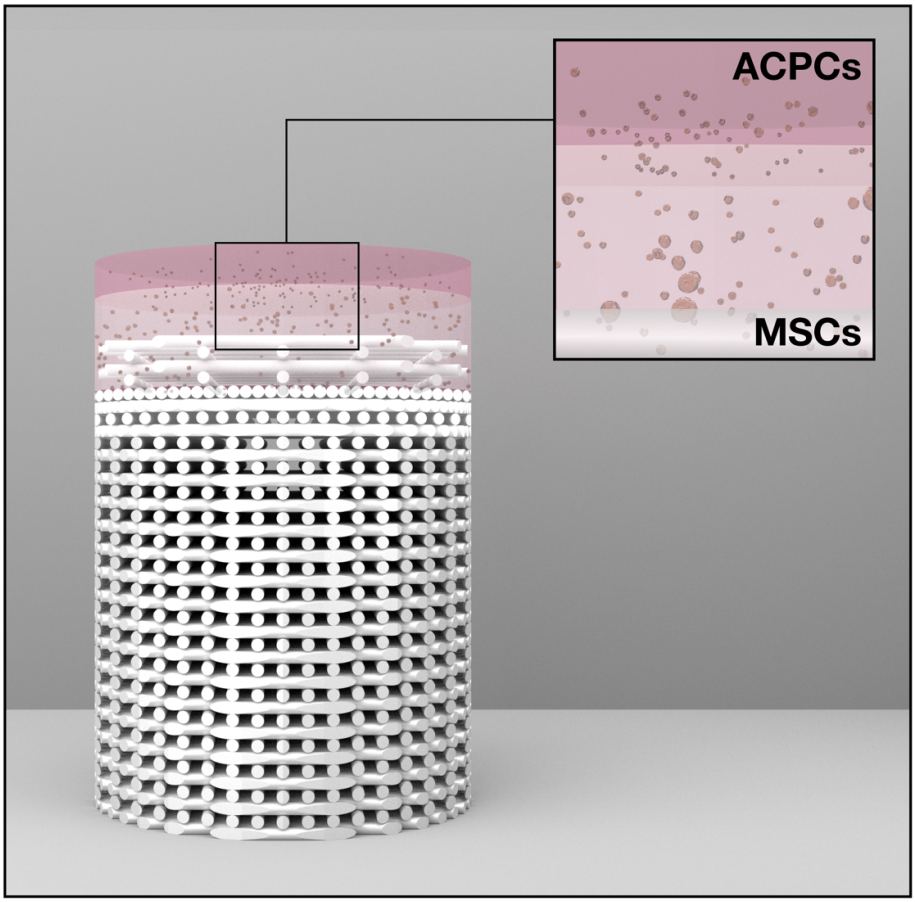

Figure 1. HA-SH/P(AGE-co-G) hydrogel/cells mixtures were cast in a layer-wise fashion on the 3D-printed PCL osteochondral scaffold. To produce the zonal constructs, the first layer of the chondral portion of the constructs was seeded with equine MSCs (35 μl, 20 $\times$ 10^6 cells ml^{-1} of hydrogel), the second with chondroprogenitor cells (ACPCs, 20 μl, 20 $\times$ 10^6 cells ml^{-1} of hydrogel).

measured after acid hydrolysis and reaction with DAB and chloramine T at 560 nm, with L-hydroxyproline as a standard. Collagen content was determined based on a hydroxyproline to collagen ratio of 1:10 [44, 45].

2.3.2. Histology and immunohistochemistry

Constructs were first fixed in 3.7% PBS-buffered formalin overnight and then, after dehydration, embedded in paraffin, and paraffin sections, 1 μm thick, were obtained. For histological analysis of GAG deposited in the constructs, sections were stained with Weigert´s hematoxylin, fast green and safranin-O [46]. For immunohistochemical analyses, antigen retrieval was performed. For aggrecan, collagen type I and collagen type II sections were treated consecutively with pronase (30 min) and hyaluronidase (30 min). Sections were blocked with 1% BSA in PBS for 60 min. For visualization, sections were stained with respective primary antibodies: anti-aggrecan (1:300, 969D4D11/AHP0022, Thermo Fisher, Waltham, USA), anti-collagen I (1:200, ab34710, Abcam, Cambridge, UK) and anti-collagen II (1:200, ab34712, Abcam, Cambridge, UK). For immunofluorescence staining, the secondary antibody Alexa Fluor 488 goat anti-rabbit IgG (1:400, 111–545-003, Jackson Immuno Research, Ely, UK) was used. For immunohistochemical staining with 3,3′-diaminobenzidine (DAB) as chromogen, the ultra streptavidin HRP detection kit (USA) (Biolegend, San Diego, USA) was used.

2.4. Long term evaluation of constructs in the equine model

A study with eight Shetland ponies was performed comparing a zonal versus a non-zonal configuration in the same animal. Zonal and non-zonal constructs were randomly implanted in either the right or left stifle joint. The study was approved by the local Ethics Committee for Animal Experimentation of Utrecht University (CCD n AVD108002015307) and was performed in accordance with the Institutional Guidelines on the Use of Laboratory Animals in compliance with the Dutch Act on Animal Experimentation.

The ponies (n = 8, age 4–10 years, weight 167–187 kg) were free of lameness and without any clinical or radiographic evidence of acute or chronic injuries. They were housed together and fed a standard maintenance ration of concentrate with hay *ad libitum* and free access to water.

General anesthesia was induced with midazolam and ketamine intravenously (0.06 and 2.2 mg kg^{-1}, respectively), after premedication with detomidine and morphine (10 mcg kg^{-1} and 0.1 mg kg^{-1}, respectively); anesthesia was maintained with isoflurane (1.1–1.5% end tidal in oxygen) with intravenous continuous rate infusion (CRI) of ketamine (0.5 mg kg^{-1} hr^{-1}) and detomidine (10 mcg kg^{-1} hr^{-1}). Furthermore, before implantation surgery all ponies received an epidural injection with morphine 0.1 mg kg^{-1} bwt in 8 ml of saline solution just before induction of anesthesia.

The medial trochlear ridge of the femoropatellar joint was exposed by arthrotomy through a subpatellar approach between the medial and middle patellar ligament; in each joint, an osteochondral defect with a diameter of 6 mm and a depth of 7.5 mm was created using a custom-made surgical drill and drill guide. After the scaffold was placed (press-fit), the wounds were closed in 4 layers using resorbable suture material (Vicryl^{TM}, Ethicon, US, LCC) and Monocryl^{TM} (Ethicon, US, LCC) for the skin. Stents were placed over the wound for protection for the first 48 h and subsequently removed. Full weight bearing was allowed after recovery from anesthesia. Postoperatively, the ponies received NSAIDS (meloxicam, 0.6 mg kg^{-1}, PO, BID-SID) up to 7 d and tramadol (5 mg kg^{-1}, PO, BID-SID) up to 3 d postoperatively. Prophylactically, antibiotics were administered perioperatively (ampicillin (10–15 mg kg^{-1}, IV), while procaine penicillin (20 mg kg^{-1}, IM) was administered once after surgery.

2.4.1. Post-operative evaluation

Orthopedic examinations were performed before surgery (baseline), and 2, 4 and 6 months after defect creation, and included objective gait analysis with a wireless networked inertial measurement system motion capture-based system (Qhorse, Qualisys AB, Göteborg, Sweden) [47]. Motion of the pelvis and protraction/retraction angle of the hindlimbs were assessed as an outcome parameter for lameness.

Second-look arthroscopy was performed at 4 and 6 months after defect creation and subsequent repair, and assessed repair tissue for attachment to surrounding articular cartilage, firmness, degree of filling and macroscopic appearance, using the Oswestry Arthroscopy Score [48].

After 6 months, animals were sedated with detomidine (10 mcg kg^{-1}) and subsequently euthanized by administration of pentobarbital (50 mg kg^{-1} of body weight). Gross assessment of the medial trochlear ridge after euthanasia consisted of evaluating the volume of the repair tissue, integration of the margins of the repair tissue with the surrounding native tissue and surface quality. After this, the entire osteochondral area of the medial femoral ridge containing the constructs was harvested for analysis using a surgical bone saw.

2.4.2. Biomechanical analysis of repair tissue

A displacement-controlled nano indenter (Piuma, Netherlands) including a controller, an optical fiber and a spherical probe (Optics, Netherlands) was used to obtain force-displacement curves on the surface of the repair tissue. The probe is attached to a spring cantilever, which is connected to the end of the optical fiber allowing to measure the cantilever deflection. A probe with radius X (54 μm) and cantilever stiffness Y (84.3 N m^{-1}) was used to perform an indentation protocol comprising an indentation phase to a depth of 18 μm for 1 s in the loading phase, followed by 7 s holding time, and an unloading time of 20 s [49]. A minimum of 3 measurements were taken at different locations within the defect, and then values were averaged.

2.4.3. Evaluation of bone repair

Each defect was scanned in a micro-CT scanner (μ-CT 80, Scanco Medical AG, Switzerland) at a resolution of 20 μm. The acquisition parameters were set to a voltage of 70 kVp, an intensity of 114 μA, and an integration time of 300 ms. Subsequently, the acquired images were processed by first applying a Gaussian filter (sigma = 2, support = 0.8 voxel) and then segmentation. The images obtained were processed with BoneJ (a free plugin of ImageJ) to obtain the bone volume fraction (BV/TV) in the defect.

2.4.4. Parenting DNA analysis

Full-thickness biopsies of repair tissue were obtained post-mortem and frozen at −20 °C. DNA was extracted using the Kleargene spin plate according to the manufacturer's instructions (LGC, UK). The PCR of 17 equine STR markers was performed according to van de Goor *et al* [50] by VHL Genetics, Wageningen, the Netherlands. Markers were compared between donor cells and host cells to detect possible presence of donor cell DNA at 6 months.

2.4.5. Histology

The osteochondral tissue blocks containing the defects were fixated in 4% formalin, decalcified with Formical-2000 (EDTA/formic acid; Decal Chemical Corporation, Tallman, NY) for 14 d, dehydrated through a graded ethanol series, cleared in xylene and then embedded in paraffin. Samples were sectioned into 5 μm slices and stained with hematoxylin and eosin (HE) and Safranin-O. Repair was assessed by a modified O'Driscoll scoring and ICRS scoring [51], and cell infiltration evaluated using an Olympus BX51 light microscope. Samples were also stained with picrosirius red and analyzed

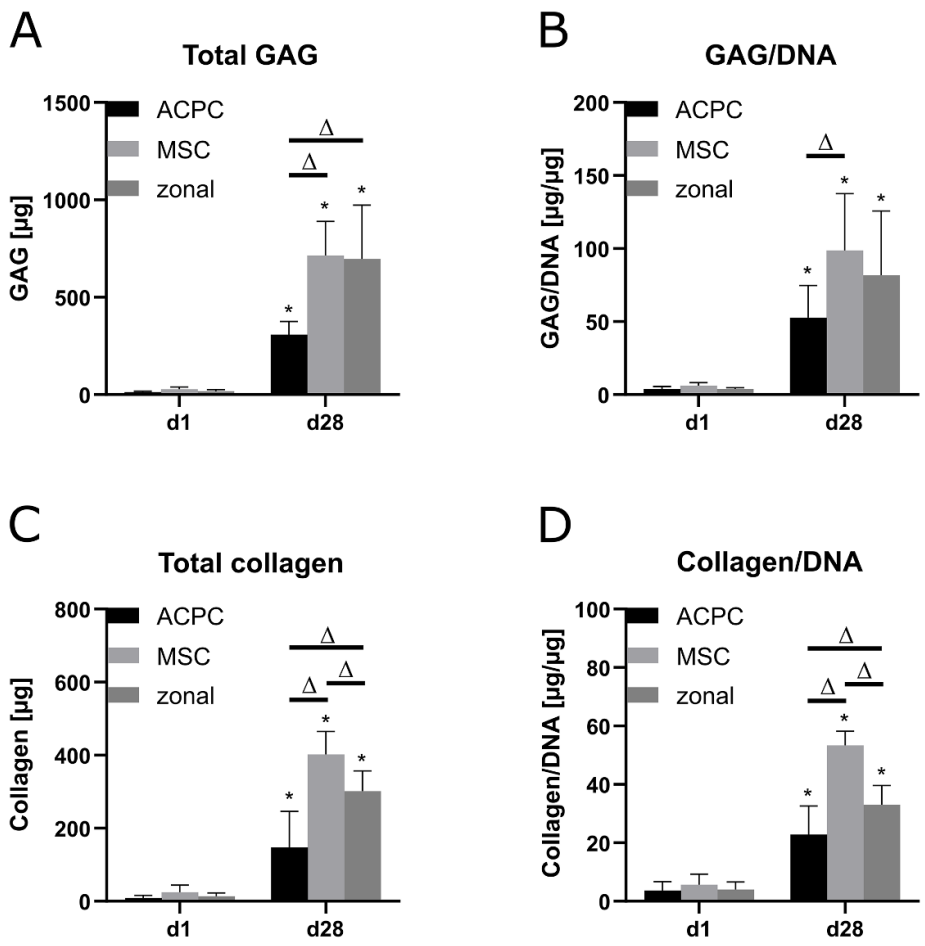

Figure 2. Biochemical analysis of ECM production in HA-SH/P(AGE-co-G) hydrogel constructs, seeded with 20.0×10^6 cells ml^{-1}, after 1 and 28 d of chondrogenic differentiation. (A) Production of total GAG (GAG/construct); (B) GAG normalized to DNA (GAG/DNA); (C) production of total collagen (collagen/construct); (D) collagen normalized to DNA (collagen/DNA). Three independent experiments with n = 3 biological replicates each were performed. Data are presented as means ± standard deviation. (*) indicates statistically significant differences between a d28 value and the corresponding d1 value of the same group ($p < 0.05$). (Δ) indicates statistically significant differences between groups ($p < 0.05$).

with polarized light microscopy for visualization of collagen fibril orientation. Immunohistochemical staining was performed for collagen type-I and type-II.

2.5. Statistical analysis

Statistical analysis for *in vitro* evaluation was performed using Graph Pad Prism 6.0 (GraphPad Software, La Jolla, USA) by two-way ANOVA with a Tukey´s post-hoc test. Differences between experimental groups were considered statistically significant at $p < 0.05$.

Statistical analysis for *in vivo* study was performed by means of the statistical package SPSS (version 25.0, IBM, Armonk, NY), using one-way ANOVA, comparing zonal and non-zonal constructs (statistical significance set at $p < 0.05$).

Statistical analysis for objective gait analysis was performed in R [52] using linear mixed models with horse used as a random effect and time as a fixed effect. Significance was set at $p < 0.05$ and correction for multiple comparison was done using the false discovery rate method'.

3. Results

3.1. *In vitro* study

3.1.1. Biochemical analysis

Within 28 d of *in vitro* culture, ACPCs and MSCs alone, as well as combined in zonal constructs were able to produce distinct amounts of GAGs within HA-SH/P(AGE-co-G) hydrogels. MSCs produced significantly more GAGs than ACPCs (figures 2(A) and (B). In line, collagen production was also observed within all constructs, with higher collagen content for MSCs compared to ACPCs (figures 2(C) and (D). Zonal layering of ACPCs and MSCs did not result in higher ECM levels compared to non-zonal constructs.

3.1.2. Histological analysis

GAG deposition was observed in all constructs. In line with the biochemical analysis, MSC-laden constructs showed more intense GAG staining than ACPC-laden constructs. This difference was also reflected in the zonal constructs, with stronger staining in the MSC-containing bottom part. In all

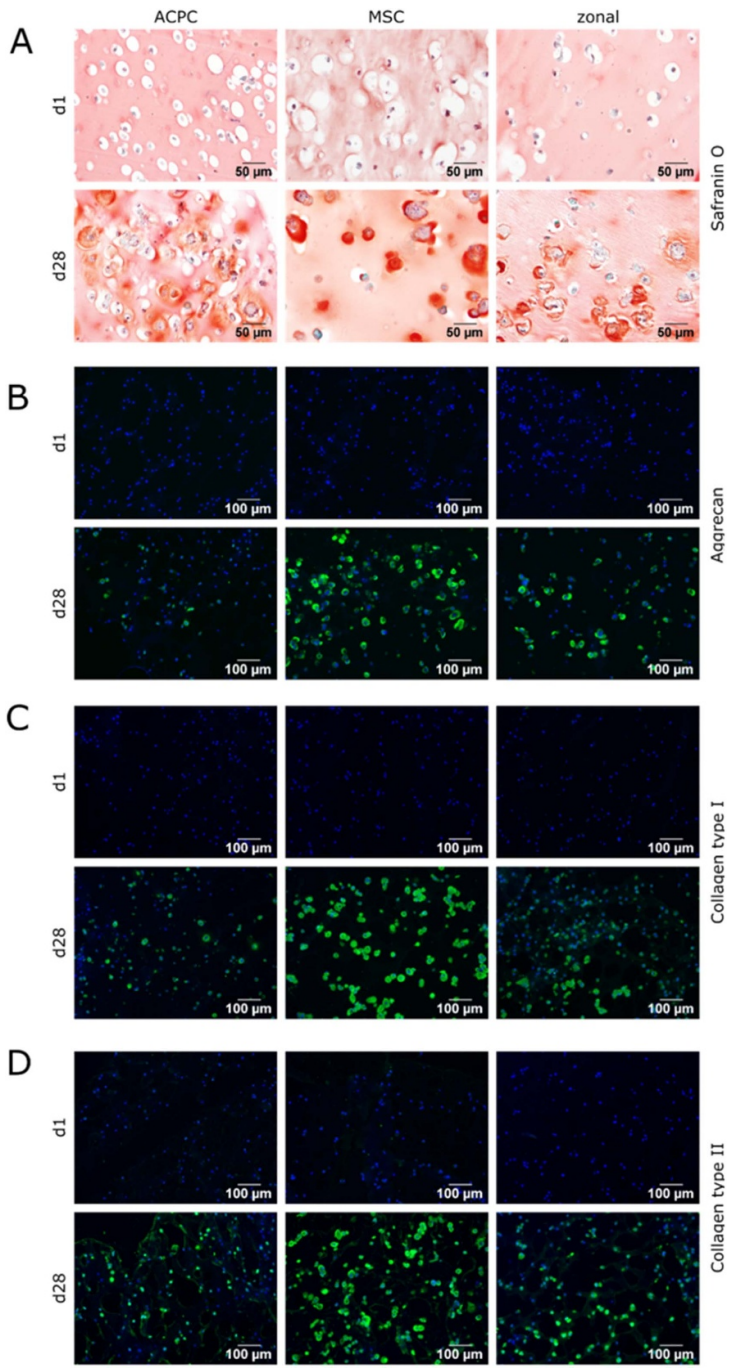

Figure 3. Histological and immunofluorescence stainings of (HA-SH/P(AGE-co-G)) hydrogel constructs, seeded with 20×106 cells ml^{-1}, after 1 and 28 d of chondrogenic differentiation. (A) Safranin O staining for GAG. Immunofluorescence stainings for (B) aggrecan, (C) collagen type I and (D) collagen type II. Three independent experiments with $n = 3$ biological replicates each were performed. Representative data from one experiment is shown. Scale bars represent 100 μm.

constructs, GAGs were mainly observed in pericellular regions, i.e. not homogeneously distributed throughout the entire construct (figure 3(A)). Similar observations were made in the immunofluorescence and immunohistochemical stainings for aggrecan and collagen types I and II (figures 3(B)–(D); figures S1, S2, Supporting Information (available online at stacks.iop.org/BF/V/A/mmedia)). High magnification of hydrogel constructs showed matrix intra- and mainly pericellularly distributed around the cells (figures S3, Supporting Information). In general, it was observed that ACPCs preferentially produced extracellular matrix in the outer areas of the constructs, whereas MSCs produced matrix within the whole construct (figures S2, Supporting Information).

3.2. Long term evaluation of constructs in the equine model

3.2.1. Post-operative evaluation

Clinical examinations after surgery did not reveal evident signs of lameness or joint effusions. All

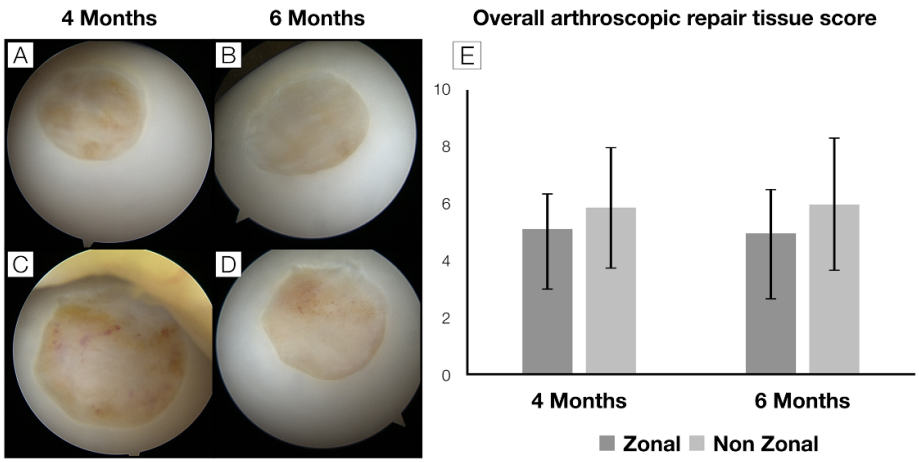

Figure 4. Arthroscopic images of representative defects at 4 and 6 months (top zonal, bottom non-zonal constructs). (A), (C) At 4 and 6 months, repair tissue filled all defects, appearing well integrated with the surrounding cartilage. (B), (D) Appearance of repair tissue changed from transparent to more whiteish over time. (E) Semi-quantitative scoring according to the oswestry arthroscopy score showed similar results for overall repair tissue quality in both groups, with no significant changes between 4 and 6 months.

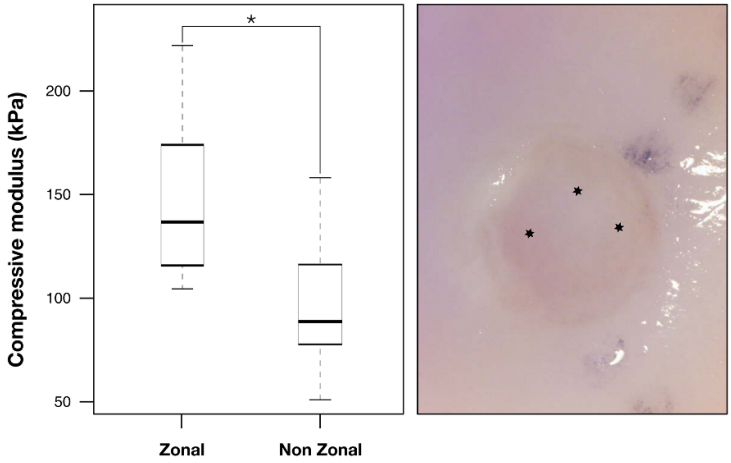

Figure 5. Biomechanical characterization of newly formed tissue filling the defects with micro-indentation. Average value of the compressive modulus in the zonal group was 147.5 ± 40.7 kPa, while in the defects repaired with non-zonal constructs, the average compressive modulus was significantly lower (96.9 ± 33.0 kPa, $p < 0.05$). A minimum of 3 measurements were performed in different areas of the defect for each animal (n = 8, right, black stars).

wounds healed by primary intention without complications.

Objective gait analysis was performed with the motion capture-based QHorse system. For both hindlimbs, maximal protraction angle was reduced after surgery and remained reduced until the last time point (5deg reduction, $p < 0.001$, figure S5(A)) Maximal retraction of the hindlimbs was initially reduced after surgery and increased over time, when compared to baseline (2.5 deg, $p < 0.001$. Figure S5(B)). Pelvis rotation along the horizontal plane (yaw) was reduced after surgery and increased at the last time point when compared to baseline (2.4deg, $p = 0.033$, figure S5(C)). Vertical motion symmetry of the pelvis in the sagittal plane reduced after surgery (1.2 mm, $p = 0.004$, figure S5(D)).

At 4 months after implantation, repair tissue filled all defects and appeared well integrated with the surrounding cartilage tissue (figures 4(A) and (C). The aspect of the repair tissue changed from transparent to more whiteish over time (figures 4(B) and (D). The semi-quantitative Oswestry scoring [48] was not different in both groups and did not show significant changes between 4 and 6 months (figure 4(E)).

3.2.2. Biomechanical analysis of the repair tissue

The average compressive modulus of the repair tissue in the zonal group was 147.5 ± 40.7 kPa. In the non-zonal constructs, this figure was significantly lower (96.9 ± 33.0 kPa, $p < 0.05$) (figure 5). Healthy cartilage from the same animals ranged at 495.9 ± 174.0 kPa.

3.2.3. Evaluation of bone repair

The bone volume fraction was similar for both groups, averaging 26.7% ± 5.6% for zonal and

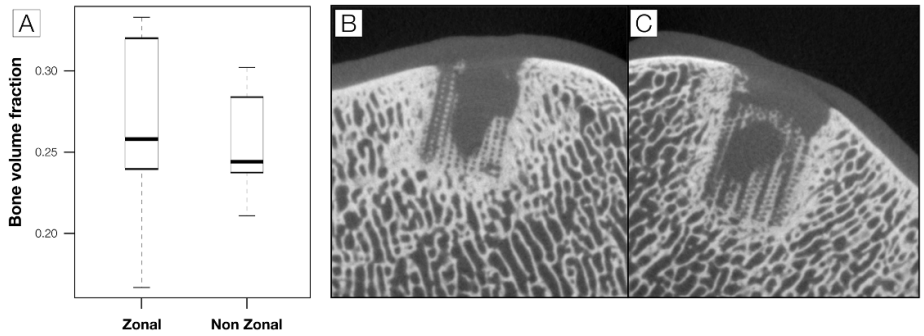

Figure 6. (A) Bone volume fraction (BV/TV) was similar for both groups, averaging 26.7% ± 5.6% for zonal and 25.7% ± 3.4% for non-zonal constructs (n = 8). (B zonal, C non-zonal) Micro-CT images of representative samples showing integration of the scaffold with the surrounding native tissue, and production of new mineralized tissue within the scaffold.

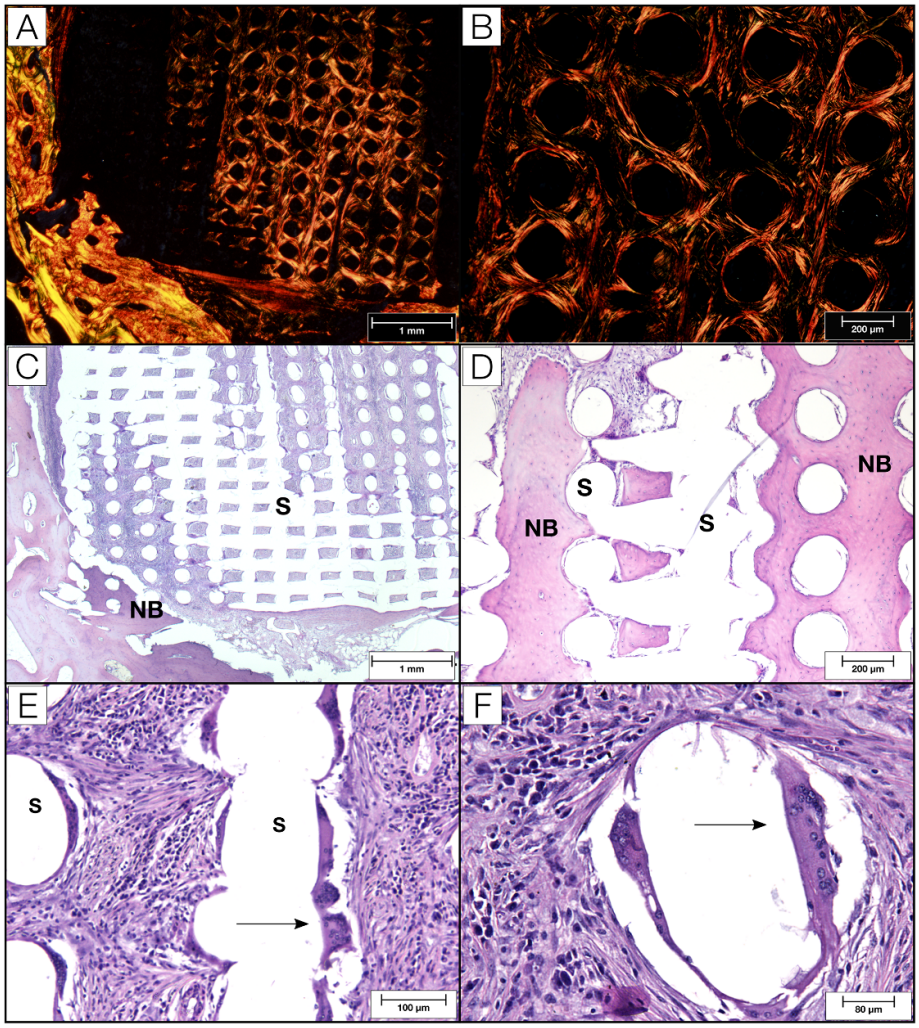

Figure 7. (A), (B) Polarized light microscopic histological images of the osteoal portion of the scaffold stained with picro-sirius red, showing presence of collagen fibers throughout. (C), (D) Hematoxylin eosin staining showed infiltration of the scaffold (S, empty space left after dissolution during histological processing) with new bone-like tissue (NB). (E), (F) At higher magnification lying along the PCL fibers of the scaffold multinucleated cells could be observed (black arrows).

25.7% ± 3.4% for non-zonal groups. (figure 6(A)). Micro-CT revealed good integration of the scaffold with the surrounding native tissue, and presence of mineralized tissue within the scaffold (figures 6(B) and (C).

Polarized light microscopy showed presence of collagen fibers throughout the osteal portion of the scaffold (figures 7(A) and (B).

Histology showed new tissue formation in construct pores with a bone-like structure (figures 7(C)

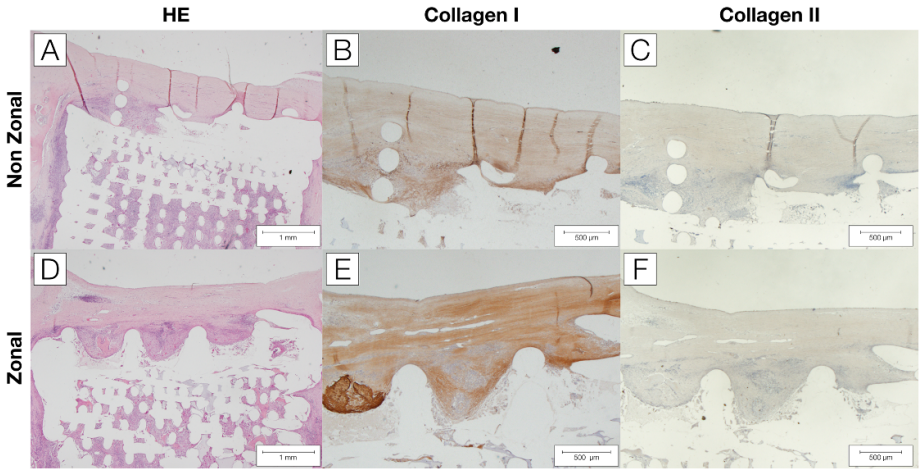

Figure 8. (A), (D) Histological sections stained with hematoxylin-eosin showing repair tissue level with the surrounding tissue, and integration with the native bone and cartilage. (B), (E) Immuno-histological staining showing widespread production of collagen I, but scarce to none presence of collagen type II, independent of zonal or non- zonal configuration (C), (F).

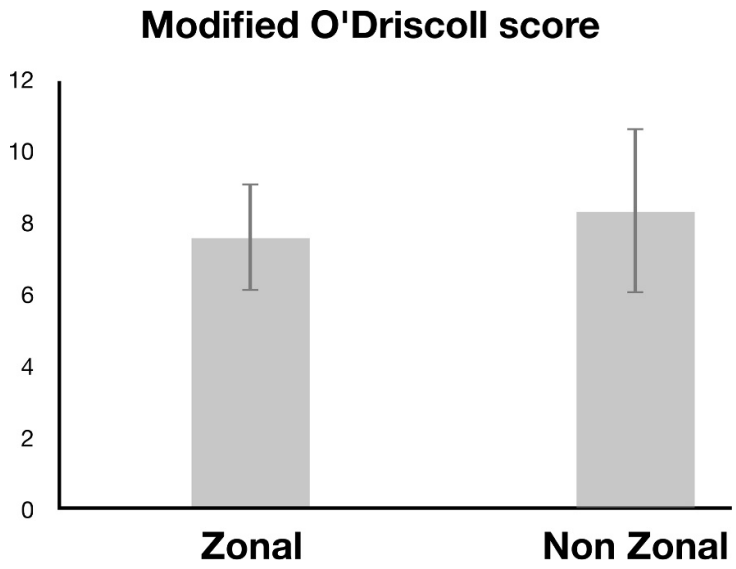

Figure 9. Microscopic scoring according to a modified O'Driscoll score did not show significant differences between the groups (n = 8).

and (D), and presence of multinucleate cells along the PCL fibers (figures 7(E) and (F)).

3.2.4. Evaluation of chondral repair tissue

Six months after surgery all defects were filled with tissue with heterogeneous appearance, suggesting a varying degree of repair tissue production. Traces of hydrogel fragments were detected. Histological analysis showed that the defect was filled with repair tissue level to the surrounding tissue, and well-integrated with the native bone and cartilage (figures 8(A) and (D)). Immuno-histological staining characterized the tissue as prevalently fibrous (figures 8(B) and (E)) with scarce to none presence of collagen type II, independently of zonal or non-zonal configuration (figures 8(C) and (F)). Staining for collagen type I appeared consistently more intense in the zonal group. Semi-quantitative histological scoring of the repair tissue did not show significant differences between zonal and non-zonal constructs (figure 9).

Parenting of DNA showed no evidence of DNA presence from donor cells and only host cells were detected.

4. Discussion

This study is the first to report on the long-term outcome of the use of a cell-seeded multi-composite fibre-reinforced hydrogel scaffold with a 3D printed anchor for fixation in the subchondral bone for the repair of artificially created osteochondral defects in an equine *in vivo* model, comparing a zonal versus a non-zonal configuration of the cartilage component. Overall, the results are similar to other longer term

studies on cartilage repair in large animal models or in humans: clinically satisfying (at least for the duration of the study), a macroscopically reasonable filling of the defect, but histologically formation of fibrocartilage at best, characterized by low, if any GAG content, production of collagen type I rather than type II and biomechanical properties that fall far short of those of native tissue [5, 12, 53, 54]. In the case of the current study the zonal constructs were significantly stiffer than the non-zonal constructs, but compressive stiffness was still a factor 6 or 7 less than that of native cartilage.

The combination of cell-seeded biomaterials with a 3D-printed scaffold is a versatile approach to address the challenge of osteochondral repair, enabling creation of mechanically competent scaffolds, while still allowing guidance of regeneration based on cells and hydrogels [55]. The choice of cell type may play a determining role. Previous studies have shown that chondrocytes may suffer dedifferentiation during *in vitro* expansion [56, 57], contrarily to MSCs [58]. However, MSCs tend to differentiate terminally and thereby can cause hypertrophy and partial matrix calcification in the tissue [59]. Nevertheless, they are still utilized for cartilage regeneration, particularly in combination with other cell types [24]. ACPCs on the other hand, can be expanded *in vitro* without losing their chondrogenic potential [34], and have been shown to differentiate chondrogenically without hypertrophy or matrix calcification [36], rendering them a promising cell source for cartilage regeneration.

The choice of allogeneic cells for the execution of the *in vivo* experiments, originates from the rationale that use of allogeneic cells would allow execution of a single step procedure, avoiding complications and costs related to two-step procedures that are necessary when using autologous cells [60]. In this study, allogeneic equine MSCs and ACPCs from two separate donors were seeded into HA-SH/P(AGE-co-G) hydrogels in non-zonal and zonal constructs. Equine MSCs have been cultured *in vitro* in HA-SH/P(AGE-co-G) hydrogel before and, when considering the different cultivation times, the levels of GAG/DNA and collagen/DNA were in the same range as in the present study [21]. The combination of MSCs and ACPCs in zonal constructs has also been previously investigated, although in association with a different gelatin-based biomaterial (gelMA) [24]. In that study, a comparison of zonal co-cultures between ACPCs, MSCs, and chondrocytes showed that the combination of ACPCs in the upper layer and MSCs in the lower layer outperformed the other combinations. MSCs produced highest levels of GAG/DNA, followed by ACPCs and then chondrocytes [24].

This promising data inspired us to use the same combination of cell types in HA-SH/P(AGE-co-G) hydrogels. In the present study, MSCs outperformed ACPCs in non-zonal constructs as well. A possible reason for this could be that the hydrogel -as well as the differentiation medium- was initially developed for MSCs; therefore with suitable adjustments, it may be possible to increase *in vitro* matrix production by ACPCs. Matrix production and distribution in zonal constructs reflected those of non-zonal constructs of the respective cell type, with more GAG and collagen in the lower layer (MSCs) compared to the superficial layer (ACPCs). As this distribution is similar to native cartilage structure, this approach towards a zonal construct consisting of two different cell types seemed promising for further evaluation in the animal model.

Even when *in vitro* studies show encouraging results, translation of tissue engineering strategies to relevant large animal preclinical models remains a persisting challenge [53, 61, 62]. Nevertheless, the large animal models are an indispensable step in the evaluation of any therapy for osteochondral repair [63], and among them the equine model is considered as probably the most challenging large animal model for cartilage repair [27]. Advantages of this model include accessibility of the joint, that allows for monitoring the repair process in long-term studies [27], and the fact that cartilage biochemical composition and thickness [28] and (subchondral) bone density approximate that of humans [64]. Disadvantages include high costs and immediate load-bearing after surgery [53]. An important ethical advantage is that the horse, unlike the majority of experimental animals, is a frequent orthopedic patient itself with a clear clinical need for improved treatment of joint injuries, as it naturally suffers from joint trauma and osteochondral diseases, due to its regular use as an athletic and working animal [27].

It is recognized that, when addressing scientific questions in large animal *in vivo* studies, many complex variables come into play. Answering a scientific question in a satisfactory way is a fundamental prerequisite, however the design needs to accomplish this while respecting the 3R's principles. With the goal of reducing possible influences of multiple groups (which may provide more data but potentially introduce confounding factors) while maintaining a scientifically sound design, the authors opted for a direct, intra-individual left-right comparison to investigate the influence of a dual (zonal) distribution of cells on cartilage repair, eliminating the large inter-individual variations characteristic of outbred populations.

The simultaneous investigation of cell-free scaffolds, or empty defects may be valid and interesting, but not directly pertinent to the understanding of the influence of cell zonal distribution in cartilage repair. Cell-free scaffolds represent an alternative approach to cartilage repair with its own merits and drawbacks [65, 66]. Similarly, while empty defects may represent a tempting control group, it is known from previous studies that defects of more than 4 mm of diameter will show poor regeneration, while requiring a higher

number of animals [67]. The use of an untreated control defect thus becomes dispendious from an economic perspective, and is undesirable in terms of respect of the 3Rs principles: the natural development of empty cartilage defects as little as 2 mm in diameter showed repair with fibrous, collagen I based tissue poor in proteoglycan content [6]. Previous authors have also opted for not using empty control defects, choosing for example a comparison with fibrin glue [1], which also presents some drawbacks in terms of fixation [7], or other repair strategies better suited for comparison to the aim of the study [2], including a direct comparison between two variations of a similar repair strategy [3], like in the case present here.

The use of multiple defects within the same joint would potentially allow for inclusion of multiple groups, while requiring a lower numbers of animals. Nevertheless, multiple larger defects within a single joint do feature the loss of proteoglycans in a relatively wide area around the defect, also affecting the surrounding healthy cartilage, and thus impacting on the repair potential of the evaluated treatments [68]. Apart from this, any additional defect will affect joint homeostasis and thus affect the conditions under which other defects in the joint must heal, making a multiple-defect approach methodologically questionable at least.

Based on earlier work on the fixation of constructs meant for the repair of focal cartilage lesions in the equine model [40], the choice was made for an osteochondral construct that could surgically be placed press-fit without need for further fixation. There are currently no satisfying techniques for fixating chondral constructs in the horse. In humans, fibrin glue is commonly used, however there are serious concerns with respect to its use in the horse, mainly because of immunological reasons [40], but also because of immediate post-surgical weight-bearing in the equine species. Biodegradable polydioxanone pins have been used with some success to secure cartilage flaps in horses affected by the developmental orthopaedic disease osteochondrosis [69], but these rely on the consistency of the native tissue (which is much less in hydrogel-based constructs) and would alter the architecture of 3D scaffolds [70]. The polycaprolactone osteochondral anchor that had been earlier designed and tested in short-term *in vivo* pilots [40] served its purpose well in this long-term *in vivo* study.

Previous equine studies testing biphasic osteochondral constructs commonly utilized either calcium phosphate (CaP) [53, 71, 72] or magnesium hydroxyapatite (Mg-HA) [5] for the osteal portion of the scaffold. This was the first long-term study in the horse that used polycaprolactone as the structural element of the osteal part of the scaffold. The material had, however, been used for reinforcement of scaffolds in other species [11, 73]. Polycaprolactone is a material that will degrade very slowly through hydrolysis (24–36 months) [74], and as expected no resorption was seen during the experimental period, differently from degradable CaP or HA-based constructs [53, 71, 72]. The PCL scaffold showed good integration with the surrounding bone with production of new mineralized tissue, in line with earlier reports [74]. Histology did not show presence of any inflammation, confirming the inertness of the material. Although the conclusion cannot be drawn definitively from the current data, it seems reasonable to presume that the scaffold will continue to slowly degrade and bone tissue will continue to be produced, likely leading to functional repair of the bone.

The performance of the cartilage portion of the implanted construct was less favourable than that of the osteal portion.

Interestingly however, clinically the animals did not display macroscopic signs of discomfort other than those expected from a surgical intervention; objective gait analysis showed that both the pelvis motion and limb movement seem to indicate a bilateral effect of the surgery. These results are compatible with a mild degree of bilateral lameness or disfunction although the effect may be very small and thus not clinically evident.

Although macroscopically the defects were for the major part neatly filled with repair tissue to the level of the original joint surface and no step defects of relevant size were seen, the tissue that was formed was virtually devoid of both glycosaminoglycans and collagen type II, whereas collagen type I was found in abundance. This type of repair tissue is similar to tissue commonly observed in repair of untreated osteochondral defects, or after surgical interventions such as micro-fracturing [12], and often represents the end stage of even more advanced therapies, such as ACI and MACI [12]. Apparently, the conditions *in vivo* were too far off from those that favoured chondrogenesis in the *in vitro* situation, where the two cell types as well as their combination showed both glycosaminoglycan and collagen type II production, be it at different rates.

It is important to state that the data presented here results from one possible zonal chondral approach and therefore its outcome should not be taken as representative for all possible zonal chondral strategies. Several factors may have played a role in obtaining these results and may offer the possibility to influence the outcome.

Firstly, DNA parenting showed that after 6 months no cells with DNA other than that of the host could be detected. This means that the seeded MSCs and ACPCs had all disappeared and had also failed in producing new generations of cells. From the experimental data it is not possible to determine when this happened, but evidently at 6 months post-implantation ongoing repair was realized solely by cells from the host. In that light, the fibrotic rather than hyaline character of the repair tissue may be

unsurprising, as it is the type of tissue that is generated by intrinsic repair of articular damage [12]. The main effect seen in this study was the marginally -but significant- higher stiffness of the repair tissue in the sites treated with the zonal constructs. This was not associated with tangible histological differences within the zonal and non-zonal groups, other than a subjectively higher intensity of collagen type I staining. Although interesting, these findings cannot be said to represent better repair.

Secondly, the degradation rate of the hydrogel on top of the PCL scaffold where MSCs and/or ACPCs were encapsulated should be considered. Histology showed the scattered presence of some persistent hydrogel fragments after 6 months, leading to the conclusion that at least some of the material resisted for a relatively long period. Although very early degeneration is considered a negative factor for the success of regeneration [14], little is known about what the desirable degradation profile should be. This represents a great challenge in tailoring the degradation profile of any biomaterial destined for cartilage repair and it is, therefore, difficult to rate the rather long-lasting but heterogeneous degradation profile seen in the current study. There was histological evidence that early degeneration did not happen in this case, but it can be questioned to what extent some scattered fragments are enough to still have any effect on the chondrogenic capacity of cells and whether cues to promote chondrogenic performance should not remain present for much longer. What can be deduced here is that the degradation profile was apparently prolonged enough to permit good filling of the defect, level to its surroundings, and formation of a good connection at the scaffold-cartilage interface, which can be seen as encouraging, as this integration prevents further deterioration of the native tissue [35].

A third factor, that may be related to the former two, is the severe lack of stiffness of the cell-seeded hydrogel that was used on top of the PCL structure. Both the overall biomechanical properties of the implant and the biomechanical environment within the structure as perceived by the seeded cells, in our materials approach, are evidently different from those generated by the native collagen network. Fibre-reinforcement can substantially improve stiffness compared to hydrogels alone, although it should be noted that stiffer materials shield cells from experiencing mechanical stimuli which may then hinder matrix production [75]. It has however been demonstrated before, that a significant improvement in stiffness can be achieved through a specific architecture of the PCL structure -with a high-volume percentage of the composite scaffold filled by the hydrogel [23]. This would be an obvious next step for construct design, once the fabrication of scaffolds by combining different production processes needed to integrate this into the osteochondral anchor is possible.

It can be concluded that the PCL-based osteochondral construct used in this equine long-term study was easy to handle surgically, could be well fixated, and gave promising results with respect to the regenerative capacities of its osteal portion. The cartilage part failed to generate better repair tissue than that produced by natural intrinsic healing of osteochondral defects. This may be related to early loss of the seeded cells, the degradation rate of the hydrogel or the failure to recreate an environment that biomechanically resembles native articular cartilage, and most likely by a combination of these factors. Future approaches should focus on materials tailoring to mimic the biomechanical environment for the seeded cells without impeding them to produce extracellular matrix elements because of excessive biomaterial stiffness, and on optimizing the degradation profile of the hydrogel. Pre-matured multiphasic scaffolds might be a way to address some of the issues raised in this study. Another approach could be the stimulation of ingrowth of native cells combined with providing long-lasting regenerative cues to these, e.g. by controlled release from extracellular vesicles, rather than relying on implantation of allogeneic cells. In all approaches it is nevertheless expected that the structural element of cartilage will present the biggest challenge.

Acknowledgments

The authors would like to acknowledge T Boeck for his expertise and help in preparation of hydrogels, H Weinans for his expertise on micro-CT analysis, F Abinzano for her help in preparation of the hydrogels, F Serra Bragança for his expertise and help with objective gait analysis, J C de Grauw and J P A M van Loon and their team for taking care of anesthesia of the ponies and the complete 'equine cartilage repair team' for logistics around the surgeries. The research leading to these results has received funding from the European Community's Seventh Framework Programme (FP7/2007–2013) under grant agreement 309962 (HydroZONES), the Dutch Arthritis Foundation (ReumaNL, LLP-12 and LLP-22). Furthermore, this work was supported by the Deutsche Forschungsgemeinschaft (DFG, German Research Foundation)—Project number 326998133—TRR 225 (sub-project A02).

ORCID iDs

I A D Mancini https://orcid.org/0000-0003-3726-4766
S Schmidt https://orcid.org/0000-0003-2762-8159
J Groll https://orcid.org/0000-0003-3167-8466
R Levato https://orcid.org/0000-0002-3795-3804
J Malda https://orcid.org/0000-0002-9241-7676

References

[1] Tamaddon M, Wang L, Liu Z and Liu C 2018 Osteochondral tissue repair in osteoarthritic joints: clinical challenges and opportunities in tissue engineering *Bio-Des. Manuf.* **1** 101–14

[2] Steadman J, Rodkey W and Briggs K 2002 Microfracture to treat full-thickness chondral defects: surgical technique, rehabilitation, and outcomes *J. Knee Surg.* **15** 170–6

[3] Solheim E, Hegna J, Øyen J, Austgulen O K, Harlem T and Strand T 2010 Osteochondral autografting (mosaicplasty) in articular cartilage defects in the knee: results at 5 to 9 years *Knee* **17** 84–87

[4] Torrie A M, Kesler W W, Elkin J and Gallo R A 2015 Osteochondral allograft *Curr. Rev. Musculoskelet Med.* **8** 413–22

[5] Kon E, Mutini A, Arcangeli E, Delcogliano M, Filardo G, Nicoli Aldini N, Pressato D, Quarto R, Zaffagnini S and Marcacci M 2010 Novel nanostructured scaffold for osteochondral regeneration: pilot study in horses *J. Tissue Eng. Regen. Med.* **4** 300–8

[6] Bicho D, Pina S, Reis R L and Oliveira J M 2018 *Osteochondral Tissue Engineering* (Berlin: Springer) pp 415–28

[7] Martin I, Miot S, Barbero A, Jakob M and Wendt D 2007 Osteochondral tissue engineering *J. Biomech.* **40** 750–65

[8] Jones K J, Kelley B V, Arshi A, McAllister D R and Fabricant P D 2019 Comparative effectiveness of cartilage repair with respect to the minimal clinically important difference *Am. J. Sports Med.* **47** 3284–93

[9] Sophia Fox A J, Bedi A and Rodeo S A 2009 The basic science of articular cartilage: structure, composition, and function *Sports Health* **1** 461–8

[10] Liang H, Ji T, Zhang Y, Wang Y and Guo W 2017 Reconstruction with 3D-printed pelvic endoprostheses after resection of a pelvic tumour *Bone Joint J.* **99** 267–75

[11] Groen W M, Diloksumpan P, van Weeren P R, Levato R and Malda J 2017 From intricate to integrated: biofabrication of articulating joints *J. Orthop Res.* **35** 2089–97

[12] LaPrade R F, Bursch L S, Olson E J, Havlas V and Carlson C S 2008 Histologic and immunohistochemical characteristics of failed articular cartilage resurfacing procedures for osteochondritis of the knee: a case series *Am. J. Sports Med.* **36** 360–8

[13] Khan I, Gilbert S, Singhrao S, Duance V and Archer C 2008 Cartilage integration: evaluation of the reasons for failure of integration during cartilage repair. A review *Eur. Cell Mater.* **16** 26–39

[14] Huey D J, Hu J C and Athanasiou K A 2012 Unlike bone, cartilage regeneration remains elusive *Science* **338** 917–21

[15] Lopa S and Madry H 2014 Bioinspired scaffolds for osteochondral regeneration *Tissue Eng.* A **20** 2052–76

[16] Di Luca A, Lorenzo-Moldero I, Mota C, Lepedda A, Auhl D, Van Blitterswijk C and Moroni L 2016 Tuning cell differentiation into a 3D scaffold presenting a pore shape gradient for osteochondral regeneration *Adv. Healthc. Mater.* **5** 1753–63

[17] Xu T, Binder K W, Albanna M Z, Dice D, Zhao W, Yoo J J and Atala A 2012 Hybrid printing of mechanically and biologically improved constructs for cartilage tissue engineering applications *Biofabrication* **5** 015001

[18] Balakrishnan B and Banerjee R 2011 Biopolymer-based hydrogels for cartilage tissue engineering *Chem. Rev.* **111** 4453–74

[19] Vinatier C, Mrugala D, Jorgensen C, Guicheux J and Noël D 2009 Cartilage engineering: a crucial combination of cells, biomaterials and biofactors *Trends Biotechnol.* **27** 307–14

[20] Stichler S, Jungst T, Schamel M, Zilkowski I, Kuhlmann M, Böck T, Blunk T, Teßmar J and Groll J 2017 Thiol-ene clickable poly (glycidol) hydrogels for biofabrication *Ann. Biomed. Eng.* **45** 273–85

[21] Stichler S, Böck T, Paxton N, Bertlein S, Levato R, Schill V, Smolan W, Malda J, Teßmar J, Blunk T and Groll J 2017 Double printing of hyaluronic acid/poly (glycidol) hybrid hydrogels with poly (ε-caprolactone) for MSC chondrogenesis *Biofabrication* **9** 044108

[22] Negoro T, Takagaki Y, Okura H and Matsuyama A 2018 Trends in clinical trials for articular cartilage repair by cell therapy *Regen. Med.* **3** 17

[23] Visser J, Melchels F P, Jeon J E, Van Bussel E M, Kimpton L S, Byrne H M, Dhert W J, Dalton P D, Hutmacher D W and Malda J 2015 Reinforcement of hydrogels using three-dimensionally printed microfibres *Nat. Commun.* **6** 6933

[24] Levato R, Webb W R, Otto I A, Mensinga A, Zhang Y, van Rijen M, van Weeren R, Khan I M and Malda J 2017 The bio in the ink: cartilage regeneration with bioprintable hydrogels and articular cartilage-derived progenitor cells *Acta. Biomater.* **61** 41–53

[25] Mouser V H, Levato R, Bonassar L J, D'lima D D, Grande D A, Klein T J, Saris D B, Zenobi-Wong M, Gawlitta D and Malda J 2017 Three-dimensional bioprinting and its potential in the field of articular cartilage regeneration *Cartilage* **8** 327–40

[26] Cucchiarini M, Madry H, Guilak F, Saris D, Stoddart M, Koon Wong M and Roughley P 2014 A vision on the future of articular cartilage repair *Eur. Cell Mater.* **27** 6

[27] Moran C J, Ramesh A, Brama P A, O'Byrne J M, O'Brien F J and Levingstone T J 2016 The benefits and limitations of animal models for translational research in cartilage repair *J. Exp. Orthop* **3** 1

[28] Malda J, Benders K, Klein T, De Grauw J, Kik M, Hutmacher D, Saris D, Van Weeren P and Dhert W 2012 Comparative study of depth-dependent characteristics of equine and human osteochondral tissue from the medial and lateral femoral condyles *Osteoarthr. Cartil.* **20** 1147–51

[29] Nixon A J, Begum L, Mohammed H O, Huibregtse B, O'callaghan M M and Matthews G L 2011 Autologous chondrocyte implantation drives early chondrogenesis and organized repair in extensive full-and partial-thickness cartilage defects in an equine model *J. Orthop Res.* **29** 1121–30

[30] Frisbie D, Bowman S, Colhoun H, DiCarlo E, Kawcak C and McIlwraith C 2008 Evaluation of autologous chondrocyte transplantation via a collagen membrane in equine articular defects–results at 12 and 18 months *Osteoarthr. Cartil.* **16** 667–79

[31] Wilke M M, Nydam D V and Nixon A J 2007 Enhanced early chondrogenesis in articular defects following arthroscopic mesenchymal stem cell implantation in an equine model *J. Orthop Res.* **25** 913–25

[32] Pelttari K, Winter A, Steck E, Goetzke K, Hennig T, Ochs B G, Aigner T and Richter W 2006 Premature induction of hypertrophy during in vitro chondrogenesis of human mesenchymal stem cells correlates with calcification and vascular invasion after ectopic transplantation in SCID mice *Arthritis Rheumatol.* **54** 3254–66

[33] Dowthwaite G P, Bishop J C, Redman S N, Khan I M, Rooney P, Evans D J, Haughton L, Bayram Z, Boyer S and Thomson B 2004 The surface of articular cartilage contains a progenitor cell population *J. Cell Sci.* **117** 889–97

[34] Williams R, Khan I M, Richardson K, Nelson L, McCarthy H E, Analbelsi T, Singhrao S K, Dowthwaite G P, Jones R E, Baird D M, Lewis H, Roberts S, Shaw H M, Dudhia J, Fairclough J, Briggs T and Archer C W 2010 Identification and clonal characterisation of a progenitor cell sub-population in normal human articular cartilage *PLoS ONE* **5** e13246

[35] Frisbie D D, McCarthy H E, Archer C W, Barrett M F and McIlwraith C W 2015 Evaluation of articular cartilage progenitor cells for the repair of articular defects in an equine model *JBJS* **97** 484–93

[36] McCarthy H E, Bara J J, Brakspear K, Singhrao S K and Archer C W 2012 The comparison of equine articular cartilage progenitor cells and bone marrow-derived stromal cells as potential cell sources for cartilage repair in the horse *Vet. J.* **192** 345–51

[37] Schumacher B L, Block J A, Schmid T M, Aydelotte M B and Kuettner K E 1994 A novel proteoglycan synthesized and secreted by chondrocytes of the superficial zone of articular cartilage *Arch. Biochem. Biophys.* **311** 144–52
[38] Mouser V H M, Levato R, Mensinga A, Dhert W J A, Gawlitta D and Malda J 2018 Bio-ink development for three-dimensional bioprinting of hetero-cellular cartilage constructs *Connect. Tissue Res.* **61** 137–51
[39] Mouser V H, Dautzenberg N M, Levato R, van Rijen M H, Dhert W J, Malda J and Gawlitta D 2018 Ex vivo model unravelling cell distribution effect in hydrogels for cartilage repair *Altex* **35** 65–76
[40] Mancini I A, Vindas Bolaños R A, Brommer H, Castilho M, Ribeiro A, Van Loon J P, Mensinga A, Van Rijen M H, Malda J and van Weeren R 2017 Fixation of hydrogel constructs for cartilage repair in the equine model: a challenging issue *Tissue Eng. C: Me* **23** 804–14
[41] Bock T, Schill V, Krahnke M, Steinert A F, Tessmar J, Blunk T and Groll J 2018 TGF-beta1-modified hyaluronic acid/poly(glycidol) hydrogels for chondrogenic differentiation of human mesenchymal stromal cells *Macromol. Biosci.* **18** e1700390
[42] Kim Y J, Sah R L, Doong J Y and Grodzinsky A J 1988 Fluorometric assay of DNA in cartilage explants using Hoechst 33258 *Anal. Biochem.* **174** 168–76
[43] Farndale R W, Buttle D J and Barrett A J 1986 Improved quantitation and discrimination of sulphated glycosaminoglycans by use of dimethylmethylene blue *Biochim. Biophys. Acta.* **883** 173–7
[44] Woessner J F Jr. 1961 The determination of hydroxyproline in tissue and protein samples containing small proportions of this imino acid *Arch. Biochem. Biophys.* **93** 440–7
[45] Hollander A P, Heathfield T F, Webber C, Iwata Y, Bourne R, Rorabeck C and Poole A R 1994 Increased damage to type II collagen in osteoarthritic articular cartilage detected by a new immunoassay *J. Clin. Invest.* **93** 1722–32
[46] Martin I, Obradovic B, Freed L E and Vunjak-Novakovic G 1999 Method for quantitative analysis of glycosaminoglycan distribution in cultured natural and engineered cartilage *Ann. Biomed. Eng.* **27** 656–62
[47] Bosch S, Serra Bragança F, Marin-Perianu M, Marin-Perianu R, van der Zwaag B J, Voskamp J, Back W, Van Weeren R and Havinga P 2018 EquiMoves: a wireless networked inertial measurement system for objective examination of horse gait *Sensors* **18** 850
[48] Van Den Borne M, Raijmakers N, Vanlauwe J, Victor J, De Jong S, Bellemans J and Saris D 2007 International Cartilage Repair Society (ICRS) and oswestry macroscopic cartilage evaluation scores validated for use in Autologous Chondrocyte Implantation (ACI) and microfracture *Osteoarthr. Cartil.* **15** 1397–402
[49] Moshtagh P R, Pouran B, Korthagen N M, Zadpoor A A and Weinans H 2016 Guidelines for an optimized indentation protocol for measurement of cartilage stiffness: the effects of spatial variation and indentation parameters *J. Biomech.* **49** 3602–7
[50] Van de Goor L, Van Haeringen W and Lenstra J 2011 Population studies of 17 equine STR for forensic and phylogenetic analysis *Anim. Genet.* **42** 627–33
[51] Mainil-Varlet P, Van Damme B, Nesic D, Knutsen G, Kandel R and Roberts S 2010 A new histology scoring system for the assessment of the quality of human cartilage repair: ICRSII *Am. J. Sports Med.* **38** 880–90
[52] RDevelopment C 2012 Team 2009: R: A language and environment for statistical computing (Vienna, Austria) (available at: http://www. R-project. org)
[53] Bolaños R V, Cokelaere S, McDermott J E, Benders K, Gbureck U, Plomp S, Weinans H, Groll J, van Weeren P and Malda J 2017 The use of a cartilage decellularized matrix scaffold for the repair of osteochondral defects: the importance of long-term studies in a large animal model *Osteoarthr. Cartil.* **25** 413–20
[54] Brun P, Dickinson S C, Zavan B, Cortivo R, Hollander A P and Abatangelo G 2008 Characteristics of repair tissue in second-look and third-look biopsies from patients treated with engineered cartilage: relationship to symptomatology and time after implantation *Arthritis Res. Ther.* **10** R132
[55] de Ruijter M, Ribeiro A, Dokter I, Castilho M and Malda J 2018 Simultaneous micropatterning of fibrous meshes and bioinks for the fabrication of living tissue constructs *Adv. Healthc. Mater.* **8** 1800418
[56] Caldwell K L and Wang J 2015 Cell-based articular cartilage repair: the link between development and regeneration *Osteoarthr. Cartil.* **23** 351–62
[57] Schnabel M, Marlovits S, Eckhoff G, Fichtel I, Gotzen L, Vecsei V and Schlegel J 2002 Dedifferentiation-associated changes in morphology and gene expression in primary human articular chondrocytes in cell culture *Osteoarthr. Cartil.* **10** 62–70
[58] Im G-I 2018 Tissue engineering in osteoarthritis: current status and prospect of mesenchymal stem cell therapy *BioDrugs* **32** 183–92
[59] Somoza R A, Welter J F, Correa D and Caplan A I 2014 Chondrogenic differentiation of mesenchymal stem cells: challenges and unfulfilled expectations *Tissue Eng. B: Rev.* **20** 596–608
[60] de Windt T S, Vonk L A, Slaper-Cortenbach I, van den Broek M P, Nizak R, van Rijen M H, de Weger R A, Dhert W J and Saris D B 2017 Allogeneic mesenchymal stem cells stimulate cartilage regeneration and are safe for single-stage cartilage repair in humans upon mixture with recycled autologous chondrons *Stem Cells* **35** 256–64
[61] Wei -C-C, Lin A B and Hung S-C 2014 Mesenchymal stem cells in regenerative medicine for musculoskeletal diseases: bench, bedside, and industry *Cell Transplant.* **23** 505–12
[62] Sah R L and Ratcliffe A 2010 Translational models for musculoskeletal tissue engineering and regenerative medicine *Tissue Eng. B: Rev.* **16** 1–3
[63] Hurtig M B, Buschmann M D, Fortier L A, Hoemann C D, Hunziker E B, Jurvelin J S, Mainil-Varlet P, McIlwraith C W, Sah R L and Whiteside R A 2011 Preclinical studies for cartilage repair: recommendations from the international cartilage repair society *Cartilage* **2** 137–52
[64] Chevrier A, Kouao A S, Picard G, Hurtig M B and Buschmann M D 2015 Interspecies comparison of subchondral bone properties important for cartilage repair *J. Orthop Res.* **33** 63–70
[65] Pot M W, Gonzales V K, Buma P, IntHout J, van Kuppevelt T H, de Vries R B and Daamen W F 2016 Improved cartilage regeneration by implantation of acellular biomaterials after bone marrow stimulation: a systematic review and meta-analysis of animal studies *PeerJ* **4** e2243
[66] Kon E, Roffi A, Filardo G, Tesei G and Marcacci M 2015 Scaffold-based cartilage treatments: with or without cells? A systematic review of preclinical and clinical evidence *Arthroscopy J. Arthroscopic Relat. Surg.* **31** 767–75
[67] Salonius E, Rieppo L, Nissi M J, Pulkkinen H J, Brommer H, Brünott A, Silvast T S, Van Weeren P R, Muhonen V and Brama P A 2019 Critical-sized cartilage defects in the equine carpus *Connect. Tissue Res.* **60** 95–106
[68] Sarin J K, Te Moller N C, Mancini I A, Brommer H, Visser J, Malda J, van Weeren P R, Afara I O and Töyräs J 2018 Arthroscopic near infrared spectroscopy enables simultaneous quantitative evaluation of articular cartilage and subchondral bone in vivo *Sci. Rep.* **8** 13409
[69] Nixon A, Fortier L, Goodrich L and Ducharme N 2004 Arthroscopic reattachment of osteochondritis dissecans lesions using resorbable polydioxanone pins *Equine Vet. J.* **36** 376–83
[70] Bekkers J, Tsuchida A, Malda J, Creemers L, Castelein R, Saris D B and Dhert W 2010 Quality of scaffold fixation in a human cadaver knee model *Osteoarthr. Cartil.* **18** 266–72
[71] Seo J-P, Tanabe T, Tsuzuki N, Haneda S, Yamada K, Furuoka H, Tabata Y and Sasaki N 2013 Effects of bilayer gelatin/β-tricalcium phosphate sponges loaded with

mesenchymal stem cells, chondrocytes, bone morphogenetic protein-2, and platelet rich plasma on osteochondral defects of the talus in horses *Res. Vet. Sci.* **95** 1210–6
[72] Tsuzuki N, Otsuka K, Seo J, Yamada K, Haneda S, Furuoka H, Tabata Y and Sasaki N 2012 In vivo osteoinductivity of gelatin β-tri-calcium phosphate sponge and bone morphogenetic protein-2 on an equine third metacarpal bone defect *Res. Vet. Sci.* **93** 1021–5
[73] Bothe F, Deubel A-K, Hesse E, Lotz B, Groll J, Werner C, Richter W and Hagmann S 2019 Treatment of focal cartilage defects in minipigs with zonal chondrocyte/mesenchymal progenitor cell constructs *Int. J. Mol. Sci.* **20** 653
[74] Hutmacher D W 2000 *The Biomaterials: Silver Jubilee Compendium* (Amsterdam: Elsevier) pp 175–89
[75] Mouw J K, Connelly J T, Wilson C G, Michael K E and Levenston M E 2007 Dynamic compression regulates the expression and synthesis of chondrocyte-specific matrix molecules in bone marrow stromal cells *Stem. Cells* **25** 655–63